

Accepted to APJ, published in vol. 722, p. 1030 (2010)

# Timing Measurements of the Relativistic Binary Pulsar PSR B1913+16

J. M. Weisberg

*Department of Physics and Astronomy, Carleton College, Northfield, MN 55057*

jweisber@carleton.edu

D.J. Nice

*Department of Physics, Lafayette College, Easton, PA 18042*

niced@lafayette.edu

and

J. H. Taylor

*Joseph Henry Laboratories and Department of Physics, Princeton University, Princeton,  
NJ 08544*

joe@princeton.edu

## ABSTRACT

We present results of more than three decades of timing measurements of the first known binary pulsar, PSR B1913+16. Like most other pulsars, its rotational behavior over such long time scales is significantly affected by small-scale irregularities not explicitly accounted for in a deterministic model. Nevertheless, the physically important astrometric, spin, and orbital parameters are well determined and well decoupled from the timing noise. We have determined a significant result for proper motion,  $\mu_\alpha = -1.43 \pm 0.13$ ,  $\mu_\delta = -0.70 \pm 0.13$  mas yr<sup>-1</sup>. The pulsar exhibited a small timing glitch in May 2003, with  $\Delta f/f = 3.7 \times 10^{-11}$ , and a smaller timing peculiarity in mid-1992. A relativistic solution for orbital parameters yields improved mass estimates for the pulsar and its companion,  $m_1 = 1.4398 \pm 0.0002 M_\odot$  and  $m_2 = 1.3886 \pm 0.0002 M_\odot$ . The system's orbital period has been decreasing at a rate  $0.997 \pm 0.002$  times that predicted as a result of gravitational radiation damping in general relativity. As we have shown before, this result provides conclusive evidence for the existence of gravitational radiation as predicted by Einstein's theory.

*Subject headings:* binaries: close — gravitation — gravitational waves — pulsars: individual (PSR B1913+16) — stars: fundamental parameters — stars: kinematics

## 1. Introduction

Pulsar PSR B1913+16 (PSR J1915+1606) was the first binary pulsar to be discovered (Hulse & Taylor 1975). Its 7.75-hr binary period and  $300 \text{ km s}^{-1}$  projected orbital velocity suggested that it would exhibit a rich set of potentially measurable relativistic effects, and that has turned out to be the case. Subsequent studies have shown that the pulsar’s companion must also be a neutron star. With tidal and rotational stellar distortions eliminated as complicating factors for any dynamical analysis, the system is an essentially clean laboratory for testing relativistic gravity. In this respect, the largest remaining complications depend on reference-frame accelerations related to the structure and dynamics of our Galaxy.

Over the past 35 years, we and our colleagues have timed PSR B1913+16 at Arecibo Observatory with steadily improving equipment and analysis techniques. Among the best known results are measurement of the general relativistic advance of periastron at a rate some 35,000 times that of Mercury in the solar system (Taylor et al. 1976); the effect of gravitational radiation damping, causing a measurable rate of orbital decay (Taylor et al. 1979); and detection of changes in the pulse shape, resulting from geodetic spin precession (Weisberg et al. 1989). Our results continue to be fully consistent with general relativity and have placed strong constraints on alternative, previously viable, relativistic theories of gravity (Weisberg & Taylor 1981; Taylor & Weisberg 1982, 1989; Taylor et al. 1992; Weisberg & Taylor 2002; Clifton & Weisberg 2008). The purpose of this paper is to provide our latest analysis of the pulsar and its orbit, based on timing observations from 1974 through 2006.

## 2. Observations

Our highest quality dataset consists of 7650 five-minute integrations of the pulse profile at wavelengths near 20 cm, each subsequently reduced to a topocentric time-of-arrival (TOA) measurement at Arecibo Observatory. These data span the years 1981 through 2006; earlier measurements are consistent with these but (owing to their much larger uncertainties) have little effect on the final results. In 2004 we made a special effort to observe regularly throughout the year, so as to improve quality of the astrometric results. Parameters of the observing equipment and associated measurement uncertainties are presented in Table 1.

Further details of the Princeton Mark I observing system are given by Taylor & Weisberg (1982), while the Mark II and III are described in Taylor & Weisberg (1989). The latest system, the Wideband Arecibo Pulsar Processor (WAPP), consists of four spectrometers optimized for pulsar work, each having 512 frequency channels across a 100 MHz bandwidth and synchronously accumulating the pulsar signal into 1024 phase bins across the full pulsar period.

### 3. Analysis of TOAs

Data were analyzed with the program TEMPO, using the JPL DE405 solar system ephemeris and the relativistic timing model of Damour & Deruelle (1986). The Damour-Deruelle approach is particularly desirable because it leaves open the question of the correct relativistic theory of gravity: one solves for phenomenological parameters whose precise relation to a gravitational theory can be investigated later. Further discussion of the Damour-Deruelle model and its application to binary pulsars in TEMPO can be found in Taylor & Weisberg (1989). Important quantities determined in this way include those related to the pulsar’s celestial position, spin, and orbit. The first category includes right ascension  $\alpha$ , declination  $\delta$ , proper motions  $\mu_\alpha$  and  $\mu_\delta$ , epoch  $t_0$ , pulse repetition frequency  $f$ , spindown rate  $\dot{f}$ , and a glitch epoch and frequency discontinuity  $\Delta f$ . Fitted orbital parameters include five Keplerian quantities: the projected semimajor axis of the pulsar orbit  $x \equiv a_1 \sin i$ , eccentricity  $e$ , epoch of periastron passage  $T_0$ , period  $P_b$ , and longitude of periastron  $\omega_0$ ; and the following relativistic or “post-Keplerian” parameters: average rate of periastron advance  $\langle \dot{\omega} \rangle$ , variations in gravitational redshift and time dilation  $\gamma$ , and orbital period derivative  $\dot{P}_b$ . As with most other pulsars that have been timed carefully over several decades, a number of “nuisance parameters” must also be measured to account for unmodeled long-term timing irregularities. These extra fitted terms have no clear physical interpretation beyond being somehow related to the poorly understood structure and dynamics of the spinning neutron star. Their mathematical form is somewhat arbitrary; as described further below, we have experimented with a number of higher-order time derivatives of the pulsar rotation frequency, and one additional frequency discontinuity.

#### 3.1. Astrometric and Spin Parameters

The astrometric and basic spin parameters determined from the full data set are listed in Table 2. A significant result for proper motion has been obtained for the first time. While the pulsar position is determined from the annual variation of TOAs as the Earth moves

about its orbit, proper motion is determined from a secular variation of this annual signal. Timing noise or other systematic effects can contaminate such measurements. We now believe that the previously reported value of PSR B1913+16’s proper motion (Taylor & Weisberg 1989) was biased by timing noise, a problem which was exacerbated by the concentrated but  $\sim$ biennially spaced observing campaigns frequently employed for this source. To circumvent these problems, we observed PSR B1913+16 several times over the course of calendar year 2004 to achieve thorough data coverage around the Earth’s orbit. By merging the 2004 data with observations made in 1985-1988, which also had good coverage throughout those years, we have now obtained a robust measurement of the pulsar’s proper motion. See Section 5 for further analyses of the proper motion result.

As in other pulsars, the measured spindown rate  $\dot{f}$  is assumed to be the result of an electromagnetic braking torque on the spinning, strongly magnetized neutron star. Its value is deterministic and (at the level of accuracy quoted in Table 2) independent of the span of data over which it is fitted. In addition, the pulsar experienced a well-defined “classical” glitch in May 2003. The magnitude  $\Delta f/f = 3.7 \times 10^{-11}$  of the event is smaller than almost all seen in the population of normal (not recycled) pulsars, with only some of the glitches in PSR B0355+54 having a comparably small magnitude (Melatos et al. 2008; Chukwude & Urama 2010). Ours is only the second glitch to be detected in a recycled pulsar, with the other (the smallest known among all pulsars) occurring in the millisecond pulsar PSR B1821–24 in globular cluster M28 (Cognard & Backer 2004).

The remaining timing parameters — higher-order derivatives  $\ddot{f}$ ,  $\ddot{\dot{f}}$ ,  $\dots$ , and (in some fits) another small frequency discontinuity in mid-1992 — were introduced to the timing solution in an *ad hoc* manner, in order to “whiten” the remaining post-fit residuals. Although we offer no clear or unique physical interpretation for these parameters, their combined effects are almost certainly a consequence of stochastic timing-noise processes in the neutron star interior (Cordes & Downs 1985; Arzoumanian et al. 1994; Urama et al. 2006). Unlike the case of the well-fitted May 2003 glitch, the values of these fitted parameters are not independent of the data span analyzed and cannot be expected to extrapolate the timing behavior accurately to future epochs. Identifying the mid-1992 behavior as a discrete event is highly uncertain, in part because of coarse sampling around that time. Our data can be fit almost as well by introducing several additional frequency derivatives instead of a second discrete event. Similar results were obtained by fitting multiple harmonically related sinusoids to the timing noise with the routine “FITWAVES” (Hobbs et al. 2004) of program TEMPO2 (Hobbs et al. 2006; Edwards et al. 2006), instead of the multiple frequency derivatives described above. Since we are unable to converge on a unique glitch parameter solution for the mid-1992 behavior, we do not include this event in Table 2.

### 3.2. Orbital Parameters

Fitted orbital parameters for PSR B1913+16 are listed in Table 3. As we have emphasized before (Taylor & Weisberg 1989), values for each of the Damour-Deruelle post-Keplerian parameters expected in general relativity can be expressed in terms of the Keplerian parameters and the initially unknown masses of the pulsar and its companion,  $m_1$  and  $m_2$ . The appropriate expressions for  $\langle \dot{\omega} \rangle$  and  $\gamma$  are

$$\begin{aligned} \langle \dot{\omega} \rangle &= 3 G^{2/3} c^{-2} (P_b/2\pi)^{-5/3} (1 - e^2)^{-1} (m_1 + m_2)^{2/3} \\ &= 2.113323(2) \left[ \frac{(m_1 + m_2)}{M_\odot} \right]^{2/3} \text{ deg yr}^{-1}, \end{aligned} \quad (1)$$

$$\begin{aligned} \gamma &= G^{2/3} c^{-2} e (P_b/2\pi)^{1/3} m_2 (m_1 + 2m_2) (m_1 + m_2)^{-4/3} \\ &= 0.002936679(2) \left[ \frac{m_2 (m_1 + 2m_2) (m_1 + m_2)^{-4/3}}{M_\odot^{2/3}} \right] \text{ s}. \end{aligned} \quad (2)$$

In the second line of each equation we have substituted values for  $P_b$  and  $e$  from Table 3, and used the constants  $GM_\odot/c^3 = 4.925490947 \times 10^{-6}$  s and 1 Julian yr =  $86400 \times 365.25$  s. The figures in parentheses represent uncertainties in the last quoted digit, determined by propagating the uncertainties listed in Table 3. In each case, the uncertainties are dominated by the experimental uncertainty in orbital eccentricity,  $e$ .

Eq. (1) may be solved for the total mass of the PSR B1913+16 system, yielding  $M = m_1 + m_2 = 2.828378 \pm 0.000007 M_\odot$ . The additional constraint provided by Eq. (2) permits a solution for each star’s mass individually,  $m_1 = 1.4398 \pm 0.0002 M_\odot$  and  $m_2 = 1.3886 \pm 0.0002 M_\odot$ . As far as we know, these are the most accurately determined stellar masses outside the solar system. It is interesting to note that since the value of Newton’s constant  $G$  is known to a fractional accuracy of only  $1 \times 10^{-4}$ ,  $M$  can be expressed more accurately in solar masses than in grams.

### 3.3. Gravitational Radiation Damping

According to general relativity a binary star system should radiate energy in the form of gravitational waves. Peters and Matthews (1963) showed that the resulting rate of change in orbital period should be

$$\begin{aligned} \dot{P}_b^{\text{GR}} &= -\frac{192 \pi G^{5/3}}{5 c^5} \left( \frac{P_b}{2\pi} \right)^{-5/3} \left( 1 + \frac{73}{24} e^2 + \frac{37}{96} e^4 \right) (1 - e^2)^{-7/2} m_1 m_2 (m_1 + m_2)^{-1/3} \\ &= -1.699451(8) \times 10^{-12} \left[ \frac{m_1 m_2 (m_1 + m_2)^{-1/3}}{M_\odot^{5/3}} \right] \end{aligned} \quad (3)$$

Inserting values obtained for  $m_1$  and  $m_2$  and propagating uncertainties appropriately, we obtain the general relativistic predicted value

$$\dot{P}_b^{\text{GR}} = -2.402531 \pm 0.000014 \times 10^{-12}. \quad (4)$$

Equations (3) and (4) apply in the orbiting system’s reference frame. Relative acceleration of that frame with respect to the solar system barycenter will cause a small additional contribution to the observed  $\dot{P}_b$ . Damour & Taylor (1991) presented a detailed discussion of this effect and other possible contributions to  $\dot{P}_b$ . Recent progress in determining the galactic-structure parameters allows us to update the relevant quantities and compute a new value for the kinematic correction to  $\dot{P}_b$ . Using  $R_0 = 8.4 \pm 0.6$  kpc for the distance to the galactic center and  $\Theta_0 = 254 \pm 16$  km s $^{-1}$  for the circular velocity of the local standard of rest (Ghez et al. 2008; Gillessen et al. 2009; Reid et al. 2009), and  $d = 9.9 \pm 3.1$  kpc for the pulsar distance (Weisberg et al. 2008), we obtain the kinematic contribution,  $\Delta\dot{P}_{\text{b,gal}}$ :

$$\Delta\dot{P}_{\text{b,gal}} = -0.027 \pm 0.005 \times 10^{-12}. \quad (5)$$

Thus, we find the ratio of observed to predicted rate of orbital period decay to be

$$\frac{\dot{P}_b - \Delta\dot{P}_{\text{b,gal}}}{\dot{P}_b^{\text{GR}}} = 0.997 \pm 0.002. \quad (6)$$

Agreement between the observed orbital decay and the general relativistic prediction is illustrated in Fig. 2, which shows how excess orbital phase (relative to an unchanging orbit) has accumulated since the pulsar’s discovery in 1974. We note that the overall experimental uncertainty embodied in Eq. (6) is now dominated by uncertainties in the galactic parameters and pulsar distance, not the pulsar timing measurements. Even better agreement between observed and expected values of  $\dot{P}_b$  would be obtained if the true value of  $R_0$  or  $d$  were slightly smaller, or  $\Theta_0$  slightly larger. For example, observed and expected values agree if  $d = 6.9$  kpc, which is within the Weisberg et al. (2008) error envelope. It will be interesting to see whether improved future estimates of these quantities will show one or more of these conditions to be true.

#### 4. Other Relativistic Effects

Two other relativistic phenomena are potentially measurable in the PSR B1913+16 system: geodetic precession and gravitational propagation delay. Spin-orbit coupling should cause the pulsar’s spin axis to precess (Damour & Ruffini 1974; Barker & O’Connell 1975a; Barker & O’Connell 1975b), which should lead to observable pulse shape changes. Weisberg et

al. (1989) first detected such changes, which were observed and modeled further by Kramer (1998). Weisberg & Taylor (2002) and Clifton & Weisberg (2008) found that the pulsar beam is elongated in the latitude direction and becomes wider in longitude with increasing distance from the beam axis in latitude. These models suggest that in the next decade or so, precession may move the beam far enough that the pulsar will become unobservable from Earth for some decades, before eventually returning to view.

The excess propagation delay (Shapiro 1964) caused by passage of pulsar signals through the curved spacetime of the companion is largest at the pulsar’s superior conjunction. The maximum amplitude varies with time because the impact parameter at superior conjunction depends strongly on the current value of  $\omega$ . In this respect the orbital geometry was particularly unfavorable in the mid-1990s (see Damour & Taylor 1992), but in coming years the propagation delay should start to become observable. Damour & Deruelle (1986) characterize the measurable quantities as range  $r = (Gm_2/c^3)$  and shape  $s \equiv \sin i$ , of the Shapiro delay, where  $i$  is the orbital inclination. As orbital precession carries our line of sight deeper into the companion’s gravitational well, future observations should permit the robust measurement of these two parameters, and hence two additional tests of relativistic theories of gravity (Damour 2009; Esposito-Farese 2009).

## 5. Systemic Velocity

Our pulsar proper motion measurement (Section 3.1), combined with the distance estimate discussed in Section 3.3, corresponds to a transverse velocity (with respect to the solar system barycenter) of  $75 \text{ km s}^{-1}$  with a galactic position angle of  $306^\circ$ ; i.e., directed 36 degrees above the galactic plane. The  $\sim 30\%$  distance uncertainty places similar limits on velocity accuracies.

We can now estimate two components of the pulsar systemic velocity in *its own* standard of rest by combining the measured pulsar transverse velocity and distance, the solar motion with respect to our Local Standard of Rest (Schönrich et al. 2010), and galactic quantities  $R_0$  and  $\Theta_0$ . The third component of motion, which is inaccessible via proper motion measurements, lies close to the direction of Galactic rotation at the pulsar’s position.

The pulsar’s galactic planar and polar velocity components relative to its standard of rest are  $247 \text{ km/s}$  almost directly away from the galactic center and  $51 \text{ km/s}$  toward the galactic North Pole, respectively. (This is significantly larger than the measured velocity in the solar system barycenter frame because the pulsar’s standard of rest velocity fortuitously cancels much of the pulsar’s peculiar velocity with respect to it.) The systemic velocity

of B1913+16 is significantly larger than other well-measured double neutron star binary system velocities, including the J0737-3037 (transverse velocity 10 km/s; Stairs et al. 2006), J1518+4905 (transverse velocity 25 km/s; Janssen et al. 2008), and B1534+12 (transverse velocity 122 km/s; Thorsett et al. 2005) systems.

## 6. Conclusions

We have analyzed the full set of Arecibo timing data on pulsar B1913+16 to derive the best values of all measurable quantities. A significant proper motion has finally been determined. A small glitch was observed in the pulsar’s timing behavior, the second known glitch in the population of recycled pulsars. The measured rate of orbital period decay continues to be almost precisely the value predicted by general relativity, providing conclusive evidence for the existence of gravitational radiation. Uncertainties in galactic accelerations now dominate the error budget in  $\dot{P}_b$ , and are likely to do so until the pulsar distance can be measured more accurately. We expect that the Shapiro gravitational propagation delay will yield additional tests of relativistic gravity within a few more years.

The three authors gratefully acknowledge financial support from the US National Science Foundation. Arecibo Observatory is operated by Cornell University under cooperative agreement with the NSF. We thank Joseph Swiggum for assistance with analyses of glitches in the pulsar population; and C. M. Ewers<sup>1</sup>, A. de la Fuente, J.T. Green, and Z. Pei for assistance with observations.

## REFERENCES

- Arzoumanian, Z., Nice, D. J., Taylor, J. H., & Thorsett, S. E. 1994, *ApJ*, 422, 671
- Barker, B. M., & O’Connell, R. F. 1975a, *Phys. Rev. D*, 12, 329
- Barker, B. M., & O’Connell, R. F. 1975b, *ApJ*, 199, L25
- Chukwude, A. E., & Urama, J. O. 2010, *MNRAS*, 910, in press
- Clifton, T., & Weisberg, J. M. 2008, *ApJ*, 679, 687
- Cognard, I., & Backer, D. C. 2004, *ApJ*, 612, L125

---

<sup>1</sup>Deceased



- Cordes, J. M., & Downs, G. S. 1985, *ApJS*, 59, 343
- Damour, T., & Ruffini, R. 1974, *Academie des Sciences Paris Comptes Rendus Serie Sciences Mathematiques*, 279, 971
- Damour, T. & Deruelle, N. 1986, *Ann. Inst. H. Poincare (Phys. Theorique)*, 44, 263
- Damour, T., & Taylor, J. H. 1991, *ApJ*, 366, 501
- Damour, T., & Taylor, J. H. 1992, *Phys. Rev D*, 45, 1840
- Damour, T. 2009, in *Physics of Relativistic Objects in Compact Binaries: From Birth to Coalescence*, eds. M. Colpi, U. Moschella, P. Casella, A. Possenti, & V. Gorini; Springer Netherlands. *Astrophysics and Space Science Library*, 359, 1; preprint available at arXiv:0707.0749 [gr-qc]
- Edwards, R. T., Hobbs, G. B., & Manchester, R. N. 2006, *MNRAS*, 372, 1549
- Esposito-Farese, G. 2009, arXiv:0905.2575 [gr-qc]
- Ghez, A. M., et al. 2008, *ApJ*, 689, 1044
- Gillessen, S., Eisenhauer, F., Trippe, S., Alexander, T., Genzel, R., Martins, F., & Ott, T. 2009, *ApJ*, 692, 1075
- Hobbs, G., Lyne, A. G., Kramer, M., Martin, C. E., & Jordan, C. 2004, *MNRAS*, 353, 1311
- Hobbs, G. B., Edwards, R. T., & Manchester, R. N. 2006, *MNRAS*, 369, 655
- Hulse, R. A., & Taylor, J. H. 1975, *ApJ*, 195, L51
- Janssen, G. H., Stappers, B. W., Kramer, M., Nice, D. J., Jessner, A., Cognard, I., & Purver, M. B. 2008, *A&A*, 490, 753
- Kramer, M. 1998, *ApJ*, 509, 856
- Melatos, A., Peralta, C., & Wyithe, J. S. B. 2008, *ApJ*, 672, 1103
- Peters. P. C., and Mathews, J. 1963, *Phys Rev*, 131, 435
- Reid, M. J., et al. 2009, *ApJ*, 700, 137
- Schönrich, R., Binney, J., & Dehnen, W. 2010, *MNRAS*, 403, 1829
- Shapiro, I. I. 1964, *Phys. Rev. Lett.*, 13, 789

- Stairs, I. H., Thorsett, S. E., Dewey, R. J., Kramer, M., & McPhee, C. A. 2006, *MNRAS*, 373, L50
- Taylor, J. H., Hulse, R. A., Fowler, L. A., Gullahorn, G. E., & Rankin, J. M. 1976, *ApJ*, 206, L53
- Taylor, J. H., Fowler, L. A., & McCulloch, P. M. 1979, *Nature*, 277, 437
- Taylor, J. H., & Weisberg, J. M. 1982, *ApJ*, 253, 908
- Taylor, J. H., & Weisberg, J. M. 1989, *ApJ*, 345, 434
- Taylor, J. H., Wolszczan, A., Damour, T., & Weisberg, J. M. 1992, *Nature*, 355, 132
- Thorsett, S. E., Dewey, R. J., & Stairs, I. H. 2005, *ApJ*, 619, 1036
- Urama, J. O., Link, B., & Weisberg, J. M. 2006, *MNRAS*, 370, L76
- Weisberg, J. M., & Taylor, J. H. 1981, *General Relativity and Gravitation*, 13, 1
- Weisberg, J. M., Romani, R. W., & Taylor, J. H. 1989, *ApJ*, 347, 1030
- Weisberg, J. M., & Taylor, J. H. 2002, *ApJ*, 576, 942
- Weisberg, J. M., Stanimirović, S., Xilouris, K., Hedden, A., de la Fuente, A., Anderson, S. B., & Jenet, F. A. 2008, *ApJ*, 674, 286

Table 1. Parameters of Observing Systems

Name	Dates	Total Bandwidth (MHz)	Frequency Channels	Time Resolution ( $\mu$ s)	TOA Uncertainty ( $\mu$ s)	Number of TOAs
Mark I . . . .	1981 – 1984	16	64	125	20	1719
Mark II . . .	1985 – 1989	8	32	125	31	1015
Mark III. . .	1988 – 2003	40	32	640	16	2473
WAPP <sup>a</sup> . . .	2003 – 2006	100	512	58	14	2443

<sup>a</sup>Three or four WAPPS were simultaneously employed in nonoverlapping frequency bands. The listed numbers refer to a single WAPP.

Table 2. Astrometric and Spin Parameters

Parameter	Value <sup>a</sup>
$t_0$ (MJD) <sup>b</sup> . . . . .	52984.0
$\alpha$ (J2000) . . . . .	$19^h15^m27^s.999928(9)$
$\delta$ (J2000) . . . . .	$16^\circ06'27''3871(13)$
$\mu_\alpha$ (mas yr <sup>-1</sup> ) . . . . .	$-1.43(13)$
$\mu_\delta$ (mas yr <sup>-1</sup> ) . . . . .	$-0.70(13)$
$f$ (s <sup>-1</sup> ) . . . . .	$16.94053778563(15)$
$\dot{f}$ (s <sup>-2</sup> ) . . . . .	$-2.4761(9) \times 10^{-15}$
Glitch epoch (MJD)	52770(20)
$\Delta f$ (s <sup>-1</sup> ) . . . . .	$6.2(2) \times 10^{-10}$

<sup>a</sup>Figures in parentheses represent estimated uncertainties in the last quoted digit. The estimated uncertainties range from  $(3 - 10) \times$  the formal fitted uncertainties, in order to also reflect variations resulting from different assumptions regarding timing noise, etc.

<sup>b</sup>This quantity is the epoch of the next six measurements tabulated here.

Table 3. Orbital Parameters

Parameter	Value <sup>a</sup>
$T_0$ (MJD) . . . . .	52144.90097841(4)
$x \equiv a_1 \sin i$ (s) . . . . .	2.341782(3)
$e$ . . . . .	0.6171334(5)
$P_b$ (d) . . . . .	0.322997448911(4)
$\omega_0$ (deg) . . . . .	292.54472(6)
$\langle \dot{\omega} \rangle$ (deg / yr) . . . . .	4.226598(5)
$\gamma$ (ms) . . . . .	4.2992(8)
$\dot{P}_b$ . . . . .	$-2.423(1) \times 10^{-12}$

<sup>a</sup>Figures in parentheses represent estimated uncertainties in the last quoted digit. The estimated uncertainties range from  $(2 - 6) \times$  the formal fitted uncertainties, in order to also reflect variations resulting from different assumptions regarding timing noise, etc.

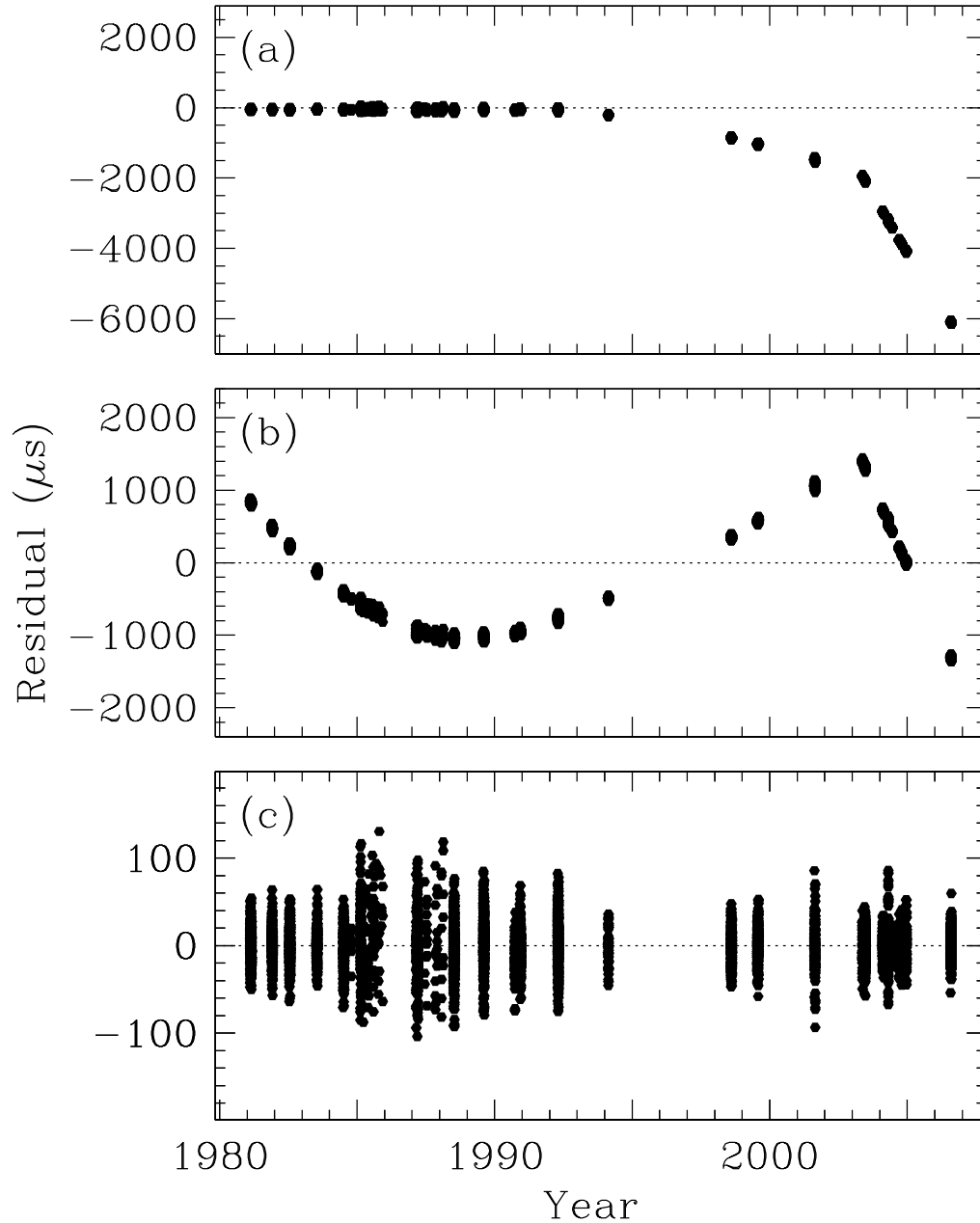


Fig. 1.— Timing residuals for PSR B1913+16. (a) Residuals from a fit for data before mid-1992. The glitch in May 2003 can be recognized by a distinct change in slope of the residuals versus time. The apparent change in mid-1992 is much smaller and may or may not involve a discrete event. (b) Residuals from a fit of all data, holding astrometric and orbital parameters fixed at the values in Tables 2 and 3; fitting for pulsar frequency and spin-down rate,  $f$  and  $\dot{f}$ ; and not allowing for higher order frequency derivatives or glitches. The glitch in May 2003 is evident as a sharp discontinuity. (c) Residuals from the full timing fit, including higher order frequency derivatives and the glitch.

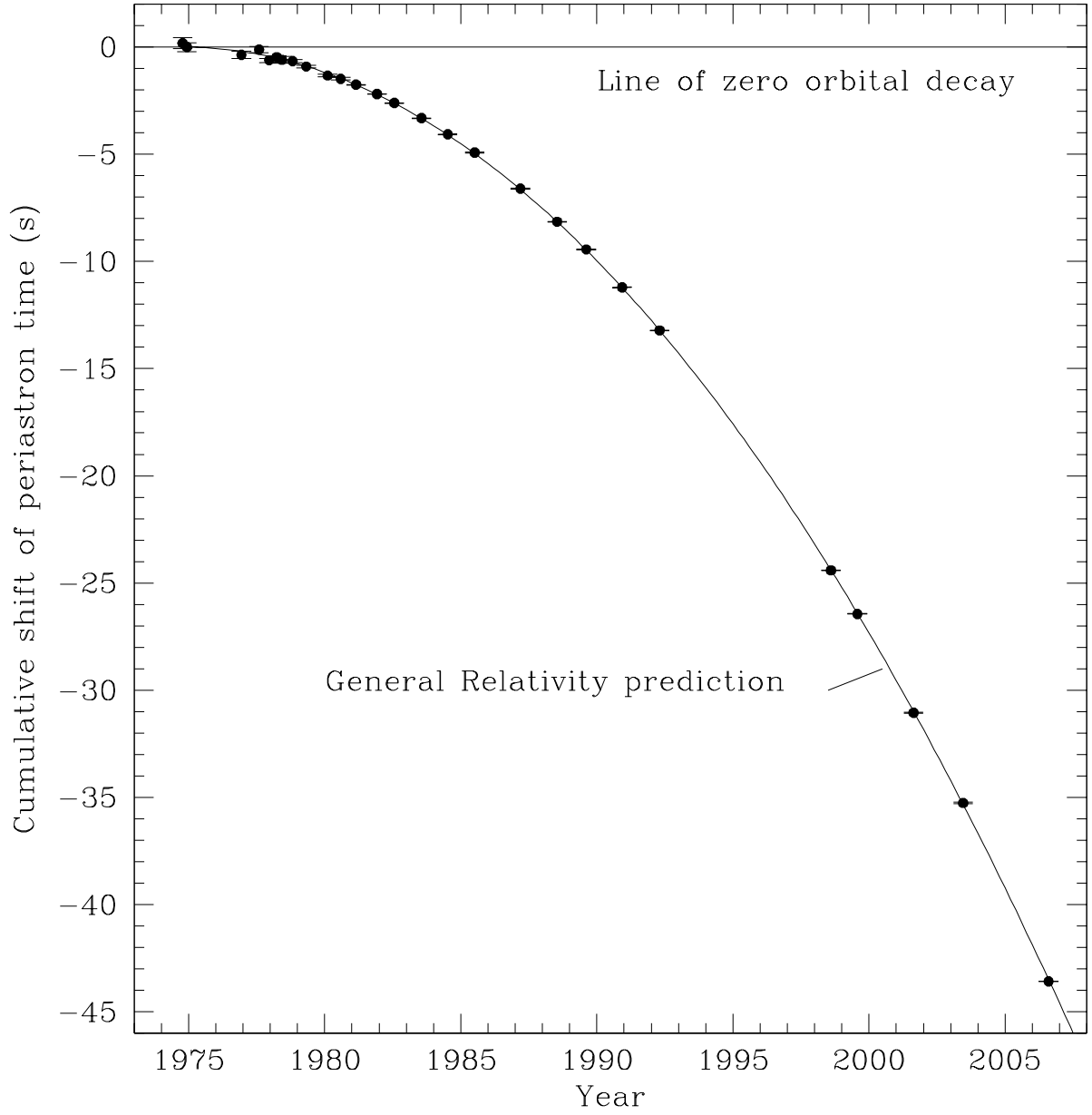


Fig. 2.— Orbital decay caused by the loss of energy by gravitational radiation. The parabola depicts the expected shift of periastron time relative to an unchanging orbit, according to general relativity. Data points represent our measurements, with error bars mostly too small to see.